A New Design Procedure for Single-Layer and Two-Layer Three-Line Baluns

Choonsik Cho, *Student Member, IEEE,* and K. C. Gupta, *Fellow, IEEE*

***Abstract*— This paper describes a design procedure for a class of three-line baluns. It is shown that the three-line balun can be considered as a combination of two identical couplers. Thus, the method developed here uses the design of couplers with an appropriate coupling factor for designing this class of baluns. The derivation leads to the normal mode parameters for the three coupled lines. Physical dimensions are obtained from these parameters. This procedure has been implemented for two-layer configurations and verified by comparison with results from a full-wave electromagnetic simulation and experimental measurement.**

***Index Terms*— Coupled lines, design methodology, multilayer circuits, three-line balun.**

I. Introduction

MANY MICROWAVE applications need the balun, which transforms a balanced transmission signal to an unbalanced transmission signal and vice versa. These applications include double-balanced mixers [1]–[5], push–pull amplifiers [6]–[8], antenna feed networks [9]–[13], frequency doublers [14]–[16], etc. A large number of balun configurations have been reported in literature. Among them, a planar version of the Marchand balun has been adapted for a long time by using microstrip lines [17]–[20], and applications of planar Marchand baluns have steadily increased in microwave integrated circuits (MIC's) and microwave monolithic integrated circuits (MMIC's).

For use in MIC and MMIC, wide bandwidth and compactness of baluns are of high interest. Multilayer configurations make MIC/MMIC more compact and can exhibit wide bandwidths due to tight coupling in coupled-line compensated baluns. Besides, flexible design can be realized by using multilayer configurations.

A compact configuration of a three-line balun reported recently in literature [21] is shown in Fig. 1. This three-line balun has more compactness than planar Marchand baluns which combine two identical coupled lines with different termination. However, a design procedure for implementing three-line baluns in single-layer or two-layer geometry has not been available.

In this paper, we describe a generic approach suitable for designing this three-line balun configuration for single-layer and two-layer structures. We show that this three-line balun configuration can be represented as a combination of two identical directional couplers each consisting of a two-coupled line section. This representation is the key step in the design procedure developed. The procedure has been used for designing single-layer and two-layer three-line baluns. The approach is verified by comparing the results with full-wave simulation results. In addition, a two-layer three-line balun has been fabricated and measured to verify the design procedure developed.

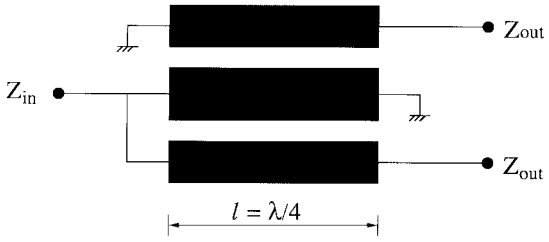

Fig. 1. The general configuration of a three-line balun.

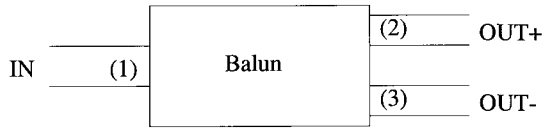

Fig. 2. The block diagram of baluns.

II. Design Procedure

A. Representation of a Balun by Two-Coupled-Line Couplers

The characteristics of baluns can be expressed in terms of the reflection coefficient ($S_{11} = 0$) and the sum of S_{21} and S_{31} ($S_{21} + S_{31} = 0$) as shown in Fig. 2 where three-port S-parameters are given by

$$[S]_{\text{Balun}} = \begin{bmatrix} 0 & -e^{-j\theta}/\sqrt{2} & e^{-j\theta}/\sqrt{2} \\ -e^{-j\theta}/\sqrt{2} & -e^{-j2\theta}/2 & -e^{-j2\theta}/2 \\ e^{-j\theta}/\sqrt{2} & -e^{-j2\theta}/2 & -e^{-j2\theta}/2 \end{bmatrix}. \quad (1)$$

This block diagram (Fig. 2) can be divided into two different blocks as shown in Fig. 3 where

$$[S]_{\text{Circuit A}} = \begin{bmatrix} 0 & -e^{-j\theta} \\ -e^{-j\theta} & 0 \end{bmatrix}$$
$$[S]_{\text{Circuit B}} = \begin{bmatrix} 0 & e^{-j\theta} \\ e^{-j\theta} & 0 \end{bmatrix}. \quad (2)$$

Manuscript received March 27, 1998; revised September 1, 1998.

The authors are with the Center for Advanced Manufacturing and Packaging of Microwave, Optical and Digital Electronics, and the Department of Electrical and Computer Engineering, University of Colorado at Boulder, Boulder, CO 80309-0425 USA (e-mail: gupta@colorado.edu; choc@colorado.edu).

Publisher Item Identifier S 0018-9480(98)09235-7.

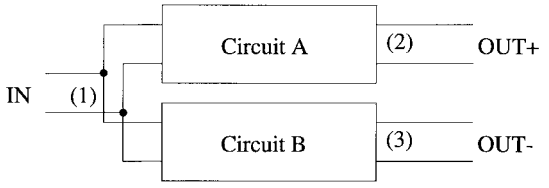

Fig. 3. The bifurcated block diagram of three-line baluns.

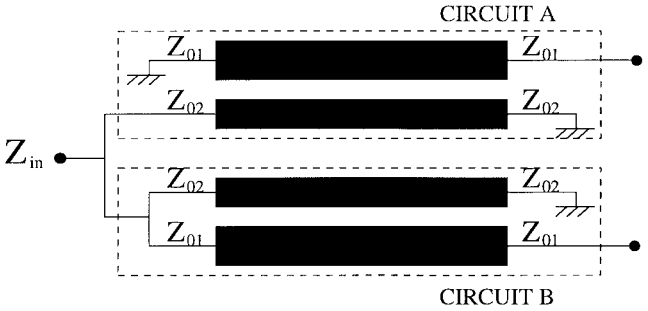

Fig. 4. A three-line balun composed of two two-line couplers.

One of the possible methods of realizing circuits A and B is by use of appropriately terminated coupled line directional couplers as shown in Fig. 4. This configuration can behave like a balun when

$$[S]_{\text{Circuit A}}(\theta = 90^\circ) = \begin{bmatrix} 0 & j \\ j & 0 \end{bmatrix}$$
$$[S]_{\text{Circuit B}}(\theta = 90^\circ) = \begin{bmatrix} 0 & -j \\ -j & 0 \end{bmatrix} \tag{3}$$

when θ is the electrical length of the two couplers.

The combination of these two two-line coupler circuits yields the following S-parameters and functions as a balun:

$$[S]_{\text{Balun}}(\theta = 90^\circ) = \begin{bmatrix} 0 & j/\sqrt{2} & -j/\sqrt{2} \\ j/\sqrt{2} & 1/2 & 1/2 \\ -j/\sqrt{2} & 1/2 & 1/2 \end{bmatrix}. \tag{4}$$

To use the design procedure for asymmetric directional couplers reported earlier [17], [22], $[Y]$ matrices for circuits A and B need to be represented in terms of the coupling factor (β) and the coupler port admittances (Y_{01}, Y_{02}) where $Y_{01} = 1/Z_{01}$, $Y_{02} = 1/Z_{02}$

$$[Y]_{\text{Circuit A}} = \begin{bmatrix} 0 & \dfrac{-j\beta\sqrt{Y_{01}Y_{02}}}{\sqrt{1-\beta^2}} \\ -j\dfrac{\beta\sqrt{Y_{01}Y_{02}}}{\sqrt{1-\beta^2}} & 0 \end{bmatrix} \tag{5}$$

TABLE I
SOME CHOICES OF Z_{01}, Z_{02} FOR BALUN INPUT/OUTPUT IMPEDANCES

$Z_{01}(\Omega)$	$Z_{02}(\Omega)$	β(Coupling factor)
38	20.42	0.367
40.825	40.825	0.5
50	100	0.707

$$[Y]_{\text{Circuit B}} = \begin{bmatrix} 0 & -j\dfrac{Y_{01} - \beta\sqrt{Y_{01}Y_{02}}}{\sqrt{1-\beta^2}} \\ -j\dfrac{Y_{01} - \beta\sqrt{Y_{01}Y_{02}}}{\sqrt{1-\beta^2}} & 0 \end{bmatrix}. \tag{6}$$

The corresponding $[S]$ matrices with the input impedance $(2Z_{\text{in}})$ and the output impedance (Z_{out}) are calculated using $[Y]$ matrices obtained in (5) and (6) as shown in (7) and (8) at the bottom of this page, where $X = 1 + \beta^2(-1 + 2Y_{01}Y_{02}Z_{\text{in}}Z_{\text{out}})$ and $Y = 1 - \beta^2 - 4\beta Y_{01}\sqrt{Y_{01}Y_{02}}Z_{\text{in}}Z_{\text{out}} + 2Y_{01}(Y_{01} + \beta^2 Y_{02})Z_{\text{in}}Z_{\text{out}}$.

Equating $[S]_{\text{Circuit A}}$ in (3) to $[S]_{\text{Circuit A}}$ in (3) and $[S]_{\text{Circuit B}}$ in (6) to $[S]_{\text{Circuit B}}$ in (8)

$$\beta = \frac{1}{2}\sqrt{\frac{Z_{02}}{Z_{01}}}. \tag{9}$$
$$Z_{02} = 4Z_{01} - \frac{2Z_{\text{in}}Z_{\text{out}}}{Z_{01}}. \tag{10}$$

We note that for a given set of balun impedances at input and output ports Z_{in} and Z_{out}, the values of coupled line parameters Z_{01} and Z_{02} are not unique. For example, when $Z_{\text{in}} = Z_{\text{out}} = 50\ \Omega$, any of the combinations shown in Table I will satisfy (9) and (10). It is found that a different choice for the values of coupler impedances (Z_{01} and Z_{02}) leads to a different bandwidth. Network simulations were carried out with two baluns, one using symmetrical directional coupler with $Z_{01} = Z_{02} = 40.825\ \Omega$, and the other with $Z_{01} = 38\ \Omega$ and $Z_{02} = 20.42\ \Omega$. S_{11} bandwidth ($|S_{11}| < -10$ dB) is 48.4%, the amplitude imbalance is within 0.91 dB, and phase error is 0° for the symmetrical case. S_{11} bandwidth is 20.9%, the amplitude imbalance is less than 1.68 dB, and phase error is 0° for the nonsymmetrical case. When we constrain $Z_{01} = Z_{02} = Z_0$, then $\beta = 0.5$ and $Z_0 = \sqrt{2Z_{\text{in}}Z_{\text{out}}/3}$.

B. Design of Three-Line Baluns

Design of the three-line balun shown in Fig. 1 is based on finding an equivalence between a six-port section of three coupled lines [shown in Fig. 5(a)] and a six-port combination

$$[S]_{\text{Circuit A}} = \begin{bmatrix} -1 + \dfrac{2(1-\beta^2)}{X} & \dfrac{j2\beta\sqrt{2(1-\beta^2)Y_{01}Y_{02}Z_{\text{in}}Z_{\text{out}}}}{X} \\ \dfrac{j2\beta\sqrt{2(1-\beta^2)Y_{01}Y_{02}Z_{\text{in}}Z_{\text{out}}}}{X} & -1 + \dfrac{2(1-\beta^2)}{X} \end{bmatrix} \tag{7}$$

$$[S]_{\text{Circuit B}} = \frac{1}{Y} \times \begin{bmatrix} 1 - \beta^2 + 4\beta Y_{01}\sqrt{Y_{01}Y_{02}}Z_{\text{in}}Z_{\text{out}} - 2Y_{01}(Y_{01} + \beta^2 Y_{02})Z_{\text{in}}Z_{\text{out}} & j2\sqrt{1-\beta^2}(-Y_{01} + \beta\sqrt{Y_{01}Y_{02}})\sqrt{2Z_{\text{in}}Z_{\text{out}}} \\ j2\sqrt{1-\beta^2}(-Y_{01} + \beta\sqrt{Y_{01}Y_{02}})\sqrt{2Z_{\text{in}}Z_{\text{out}}} & 1 - \beta^2 + 4\beta Y_{01}\sqrt{Y_{01}Y_{02}}Z_{\text{in}}Z_{\text{out}} - 2Y_{01}(Y_{01} + \beta^2 Y_{02})Z_{\text{in}}Z_{\text{out}} \end{bmatrix} \tag{8}$$

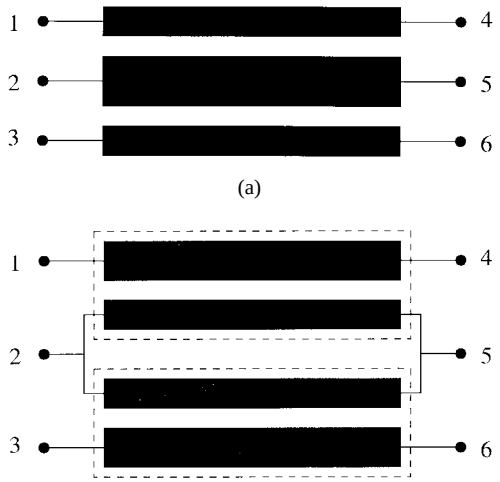

Fig. 5. Equivalence between (a) a section of three-coupled lines and (b) a six-port network combination of two couplers.

of two couplers as shown in Fig. 5(b). The normal mode parameters of the three-coupled lines shown in Fig. 5(a) can be found by equating the six-port $[Y]$ matrix of these three-coupled lines to the $[Y]$ matrix of the six-port circuit shown in Fig. 5(b). For the circuit shown in Fig. 5(b), the two sets of identical two-coupled lines shown enclosed by the dotted lines are perfectly isolated. For finding out this equivalence, three different phase velocities of the coupled line in Fig. 5(a) are assumed to be equal because a little deviation in them does not affect the balun performance seriously. This procedure leads to the following relations among the normal mode parameters (NMP) of the structure in Fig. 5(a) and the c- and π-mode parameters of two identical couplers in Fig. 5(b):

$$Y_{m1} = \frac{R_\pi Y_{c1} - R_c Y_{\pi 1}}{R_\pi - R_c} \tag{11}$$

$$\frac{Y_{p1} - Y_{n1}}{R_{V1} - R_{V2}} = \frac{Y_{c1} - Y_{\pi 1}}{R_\pi - R_c} \tag{12}$$

$$\frac{R_{V2}Y_{p1} - R_{V1}Y_{n1}}{R_{V1}R_{V2}(Y_{p1} - Y_{n1})} = \frac{R_c Y_{c1} - R_\pi Y_{\pi 1}}{R_c R_\pi (Y_{c1} - Y_{\pi 1})} \tag{13}$$

$$\frac{R_{V1}Y_{p1} - R_{V2}Y_{n1}}{Y_{p1} - Y_{n1}} = \frac{R_\pi Y_{c1} - R_c Y_{\pi 1}}{Y_{c1} - Y_{\pi 1}} \tag{14}$$

where R_{V1}, R_{V2} are the voltage ratios and Y_{m1}, Y_{n1}, Y_{p1} are the admittances of three normal modes (m, n, p modes) for three-coupled lines [23], and R_c, R_π, Y_{c1}, $Y_{\pi 1}$ are c- and π-mode voltage ratios and admittances for two-line couplers [24]. It is noted that we have only four equations (11)–(14) for five independent values (R_{V1}, R_{V2}, Y_{m1}, Y_{n1}, and Y_{p1}) of NMP of three-coupled lines. Thus, one of these parameters needs to be selected independently, and this choice will lead to different designs for the balun. These NMP for the three-line structure are used to find the geometry of the three-line balun.

C. Physical Geometry for the Three-Line Balun

Physical geometry is determined by an optimization process. This process repeatedly compares the desired NMP for three-coupled lines (evaluated as indicated in Section II-B) with NMP calculated from selected dimensions for three-coupled lines. A quasi-static field analysis program called the segmentation and boundary element method (SBEM) [22] has been used to calculate inductance and capacitance matrices for specific geometries.

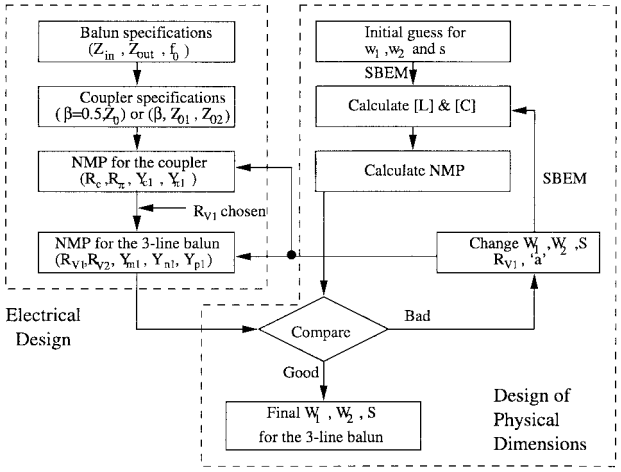

Fig. 6. A design procedure for three-line baluns.

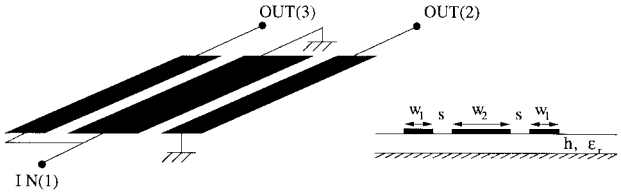

Fig. 7. The physical layout of a single-layer three-line balun.

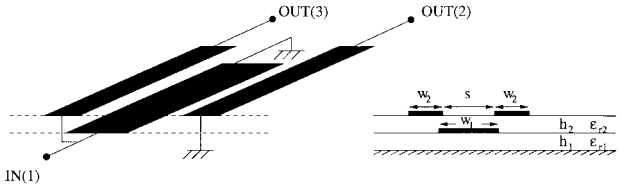

Fig. 8. The physical layout of a two-layer three-line balun (topology A).

The design procedure discussed in this section is summarized in the flow diagram of Fig. 6. The electrical design part in the left-hand column yields NMP for three-coupled lines, and the physical design part in the right-hand column leads to the physical dimensions appropriate for realizing the NMP calculated in the electrical design part.

The design is verified by simulating the optimized geometry on a full-wave electromagnetic simulator and measuring the performance of a two-layer three-line balun designed and fabricated using the design procedure reported here.

III. Design Example

We illustrate the procedure developed by an example of a single-layer three-line balun shown in Fig. 7 and two examples of two-layer three-line baluns shown in Figs. 8 and 9.

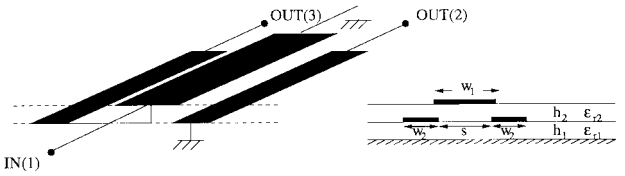

Fig. 9. The physical layout of a two-layer three-line balun (topology B).

TABLE II
PARAMETERS FOR THE DESIGN EXAMPLE OF A SINGLE-LAYER THREE-LINE BALUN

Inputs		Outputs	
h	15 mil	Z_{01}	40.825 Ω
ϵ_r	10	Z_{02}	40.825 Ω
Z_{in}	50 Ω	Coupling factor(β)	-6.0 dB
Z_{out}	50 Ω	W_1	0.348 mm
		W_2	1.086 mm
		S	0.018 mm

TABLE III
PARAMETERS FOR THE DESIGN EXAMPLE OF A TWO-LAYER THREE-LINE BALUN (TOPOLOGY A)

Inputs		Outputs	
h_1	20 mil	Z_{01}	40 Ω
h_2	20 mil	Z_{02}	35 Ω
ϵ_{r1}	2.2	Coupling factor(β)	-6.6 dB
ϵ_{r2}	2.2	W_1	4.280 mm
Z_{in}	50 Ω	W_2	3.643 mm
Z_{out}	50 Ω	S	1.710 mm
		Length(at 3 GHz)	17.749 mm

TABLE IV
PARAMETERS FOR THE DESIGN EXAMPLE OF A TWO-LAYER THREE-LINE BALUN (TOPOLOGY B)

Inputs		Outputs	
h_1	20 mil	Z_{01}	43 Ω
h_2	20 mil	Z_{02}	55.7 Ω
ϵ_{r1}	2.2	Coupling factor(β)	-4.9 dB
ϵ_{r2}	2.2	W_1	1.343 mm
Z_{in}	50 Ω	W_2	5.771 mm
Z_{out}	50 Ω	S	0.506 mm
		Length(at 3 GHz)	17.243 mm

A. Single-Layer Three-Line Baluns

Input parameters and optimized output parameters for the single-layer design example are shown in Table II. In this case, the spacings between the adjacent lines are so narrow (0.018 mm in this example) that it is difficult to fabricate this design. Therefore, we need to consider two-layer structure as an alternative.

B. Two-Layer Baluns

Input parameters and optimized output parameters for the two-layer design examples are shown in Table III and Table IV, respectively. For the three-line structure used for the balun, the wavelength is taken as the arithmetic mean of phase velocities of three normal modes divided by the design frequency.

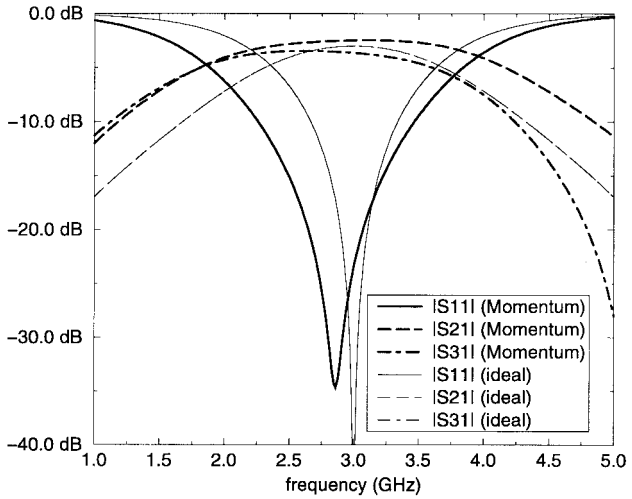

Fig. 10. The performance of two-layer three-line balun (topology A) designed by the procedure developed and comparison with an "ideal" balun.

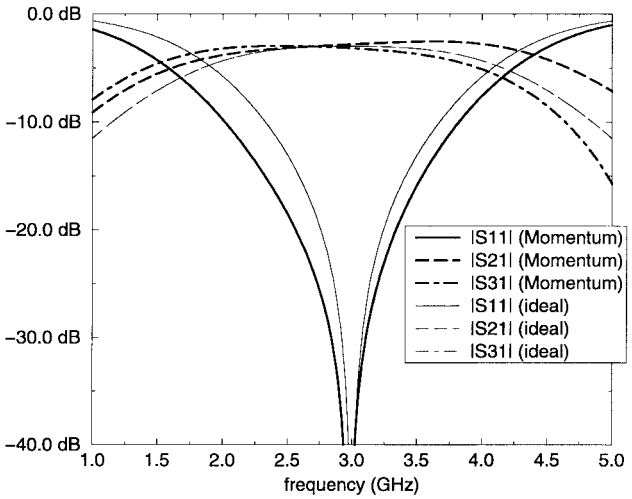

Fig. 11. The performance of two-layer three-line balun (topology B) designed by the procedure developed and comparison with an "ideal" balun.

Using the physical geometry obtained above, the two-layer three-line balun structures have been simulated on a full-wave EM simulator (HP's Momentum). S-parameters obtained from an EM simulation are compared with those for an "ideal" balun in Figs. 10 and 11. The performance of the "ideal" balun is calculated using the desired NMP and the phase velocities for the three modes assumed to be equal. Magnitudes of S-parameters are plotted in Fig. 12. The phase imbalance $(\angle S_{21} - \angle S_{31})$ is plotted in Fig. 13. We note that for topology A, the center frequency is shifted to 2.86 GHz, the actual loss is -4.44 to -2.48 dB, the amplitude imbalance at the balanced output ports is within 1.96 dB, and the phase error is less than 10.4° over the frequency range of 2.26–3.45 GHz where $|S_{11}| < -10$ dB. For topology B, the center frequency is shifted to 2.98 GHz, the actual loss is -4.44 to -2.56 dB, the amplitude imbalance at the balanced output ports is within 1.88 dB, and phase error is only 0.2° over 2.14–3.78

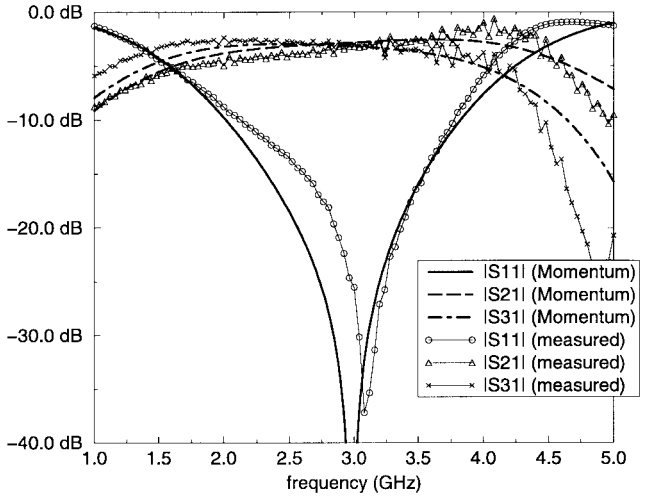

Fig. 12. The measured performance of two-layer three-line balun (topology B) designed by the procedure developed and comparison with a full-wave simulation.

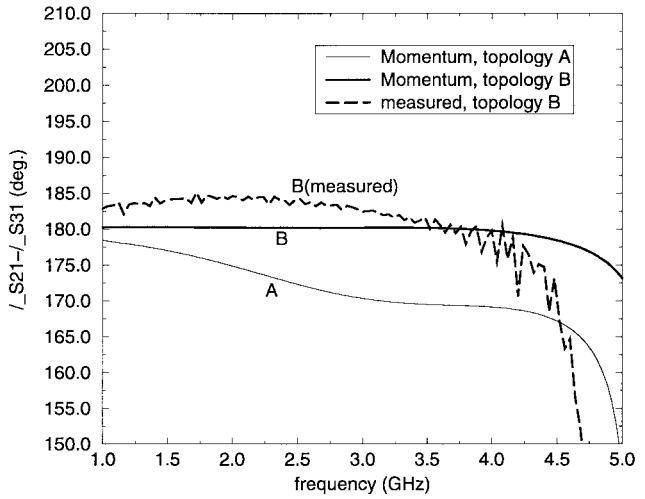

Fig. 13. The phase imbalances of two-layer three-line baluns designed by the procedure developed.

GHz where $|S_{11}| < -10$ dB. Thus, we note that topology B yields simulated performance close to the ideal performance. Moreover, by our experience, topology B allows 0.5 mm misalignment in simulation.

It may be noted that, as in other synthesis procedures at microwave frequencies, the procedure developed here does not take into account via inductances, discontinuity reactances, difference in the phase velocities of three normal modes, and dispersion in coupled lines. One needs to compensate for these effects by an optimization of the initial design obtained. However, the method developed provides an efficient tool for an initial design.

A balun using topology B was fabricated on the Duroid RT5880 substrate as shown in Fig. 14 where the input and the output ports are extended to locate connectors easily. Its performance is measured and plotted in Figs. 12 and 13. As shown in Figs. 12 and 13, the design frequency is shifted to 3.10 GHz, $|S_{11}|$ is less than -10 dB over 2.13–3.78 GHz. In this frequency range, the actual loss is -4.99 to

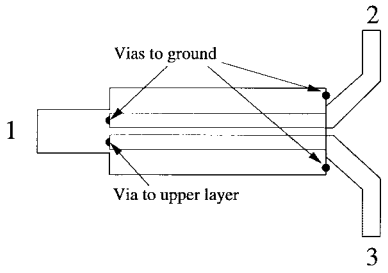

(a)

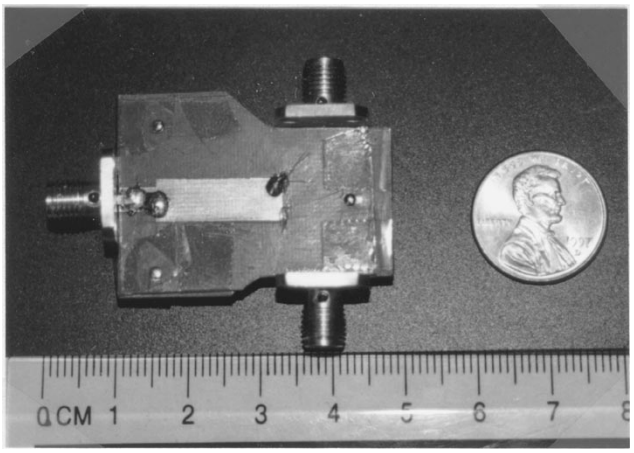

(b)

Fig. 14. (a) The layout of a two-layer three-line balun fabricated on Duroid RT5880, and (b) the photograph of a two-layer three-line balun fabricated on Duroid RT5880.

-2.2 dB, the amplitude imbalance is within 2.12 dB, and the phase error is less than 4.51°. These measurement results agree fairly well with the simulation results. Some of the possible reasons for lack of better agreement are: the air gap between two layers, the lead inductance of vias used to connect ground and two layers, nonidentical physical lengths of the two extended output ports, misalignment between two substrates, and inaccurate calibration process (because of input and output connections at different levels).

IV. Concluding Remarks

A design procedure for the three-line balun using the design of a coupler has been presented. The analytical procedure yields normal mode parameters for the coupled lines. Physical dimensions are obtained by optimization using a quasi-static analysis program. Alternatively, an electromagnetic artificial neural network (EM-ANN) model could be developed for this procedure.

This method was verified by designing single-layer and two-layer three-line baluns. The single-layer version produces very narrow spacing between three strips, therefore, two-layer versions that provide more design flexibility have been implemented. A two-layer three-line balun was fabricated and measured to verify the design procedure. Experimental results are compared to those obtained from a full-wave EM simulation. This kind of balun showed a good performance in spite of imperfect fabrication facilities leading to a misalignment between the two substrates. Thus, this design allows

considerable flexibility in the design procedure and yields reasonable tolerances for fabrication.

REFERENCES

[1] Y. I. Ryu, K. W. Kobayashi, and A. K. Oki, "A monolithic broadband doubly balanced EHF HBT star mixer with novel microstrip baluns," *IEEE MTT-S Int. Microwave Symp. Dig.*, 1995, pp. 119–122.

[2] H. K. Chiou, C. Y. Chang, and H. H. Lin, "A uniplanar broadband double-balanced mixer using a novel balun design," in *Proc. Int. Symp. Commun.*, 1995, pp. 1221–1228.

[3] K. W. Kobayashi, L. T. Tran, M. Lammert, T. R. Block, A. K. Oki, and D. C. Streit, "A novel 12–24 GHz broadband HBT distributed active balanced mixer," in *IEEE Radio Frequency Integrated Circuits Symp. Dig.*, 1997, pp. 75–78.

[4] K. Kamozaki, N. Kurita, T. Tanimoto, H. Ohta, T. Nakamura, and H. Kondoh, "50–100 GHz octave band MMIC mixers," in *IEEE Radio Frequency Integrated Circuits Symp. Dig.*, 1997, pp. 95–98.

[5] K. Nishikawa, I. Toyoda, and T. Tokumitsu, "Miniaturized three-dimensional MMIC K-band upconverter," *IEEE Microwave Guided Wave Lett.*, vol. 7, pp. 230–232, Aug. 1997.

[6] P. C. Hsu, C. Nguyen, and M. Kintis, "Uniplanar broad-band push-pull FET amplifiers," *IEEE Trans. Microwave Theory Tech.*, vol. 45, pp. 2150–2152, Dec. 1997.

[7] W. Bischof, W. Ehrlinger, K. Haug, M. Berroth, and M. Schlechtweg, "An extremely wide band balanced amplitude controller in coplanar waveguide technology," in *Proc. 25th European Microwave Conf.*, pp. 921–925, 1995.

[8] M. N. Tutt, H. Q. Tserng, and A. Ketterson, "A low loss, 5.5 GHz-20 GHz monolithic balun," in *IEEE MTT-S Int. Microwave Symp. Dig.*, 1997, pp. 933–936.

[9] G. S. Hilton, C. J. Railton, C. J. Ball, M. Dean, and A. L. Hume, "Modeling a three-element printed dipole antenna array using the FDTD technique," in *IEEE Antennas and Propagation Society Int. Symp. Dig.*, 1997, pp. 1062–1065.

[10] Y.-D. Lin and S.-N. Tsai, "Coplanar waveguide-fed uniplanar bow-tie antenna," *IEEE Trans. Antennas, Propagat.*, vol. 45, pp. 305–306, Feb. 1997.

[11] A. Nesic and S. Dragas, "Frequency scanning printed array antenna," in *IEEE AP-S Int. Symp. Dig.*, 1995, pp. 950–953.

[12] N. I. Dib, R. N. Simons, and L. P. B. Katehi, "New uniplanar transitions for circuit and antenna," *IEEE Trans. Microwave Theory Tech.*, vol. 43, pp. 2868–2873, Dec. 1995.

[13] M. W. Nurnberger and J. L. Volakis, "A new planar feed for slot spiral antennas," *IEEE Trans. Antennas, Propagat.*, vol. 44, pp. 130–131, Jan. 1996.

[14] S. A. Maas and Y. Ryu, "A broadband, planar, monolithic resistive frequency doubler," in *IEEE MTT-S Int. Microwave Symp. Dig.*, 1994, pp. 443–446.

[15] D. F. Filipovic, R. F. Bradley, and G. M. Rebeiz, "A planar broadband MIC balanced varactor doubler using a novel grounded-CPW to slotline transition," in *IEEE MTT-S Int. Microwave Symp. Dig.*, 1994, pp. 1633–1636.

[16] R. Bitzer, "Planar broadband MIC balanced frequency doubler," in *IEEE MTT-S Int. Microwave Symp., Dig.* 1991, pp. 273–276.

[17] C. M. Tsai and K. C. Gupta, "A generalized model for coupled lines and its applications to two-layer planar circuits," *IEEE Trans. Microwave Theory Tech.*, vol. 40, pp. 2190–2198, Dec. 1992.

[18] M. Engels and R. H. Jansen, "Design of integrated compensated baluns," *Microwave Optical Tech. Lett.*, vol. 14, no. 2, pp. 75–81, Feb. 1997.

[19] R. Schwindt and C. Nguyen, "Computer-aided analysis and design of a planar multilayer marchand balun," *IEEE Trans. Microwave Theory Tech.*, vol. 42, pp. 1429–1434, July 1994.

[20] R. H. Jansen, J. Jotzo, and R. Engels, "Improved compaction of multilayer MMIC/MCM baluns using lumped element compensation," in *IEEE MTT-S Int. Microwave Symp. Dig.*, 1997, pp. 277–280.

[21] C. M. Tsai and K. C. Gupta, "CAD procedures for planar re-entrant type couplers and three-line baluns," in *IEEE MTT-S Int. Microwave Symp. Dig.*, 1993, pp. 1013–1016.

[22] ———, "Field analysis, network modeling and circuit applications of inhomogeneous multi-conductor transmission lines," Research Center for Microwave and Millimeter-wave Computer Aided Design, Univ. Colorado at Boulder, Tech. Rep. 19, Dec. 1993.

[23] V. K. Tripathi, "On the analysis of symmetrical three-line microstrip circuits," *IEEE Trans. Microwave Theory Tech.*, vol. MTT-25, pp. 726–7292, Sept. 1977.

[24] ———, "Asymmetric coupled transmission lines in an inhomogeneous medium," *IEEE Trans. Microwave Theory Tech.*, vol. MTT-23, pp. 734–739, Sept. 1975.

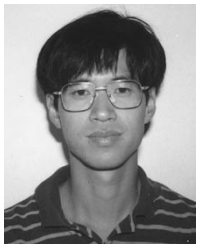

Choonsik Cho (S'98) was born in the Republic of Korea. He received the B.S. degree in control and instrumentation engineering from Seoul National University, Seoul, Korea, in 1987 and the M.S. degree in electrical and computer engineering from the University of South Carolina, Columbia, in 1995. Since then, he has been working toward the Ph.D. degree in electrical and computer engineering at the University of Colorado at Boulder.

His principal research interest is the design of multilayer microwave circuits.

K. C. Gupta (M'62–SM'74–F'88), for biography, see this issue, p. 2275.